Journal of Oceanography
Vol. 51, pp. 441 to 458. 1995

Mechanism of the Seasonal Transport Variation through the Tokara Strait

M. KUBOTA*, H. YOKOTA and T. OKAMOTO**

School of Marine Science and Technology, Tokai University, Shimizu, Shizuoka 424, Japan

(Received 18 October 1994; in revised form 27 February 1995; accepted 1 March 1995)

To investigate a mechanism of the seasonal variation of transport through the Tokara Strait, two numerical experiments with real geometry and wind forcing were carried out. The models are linear barotropic models which are a North Pacific Ocean model and a limited-area model with a fine grid. The seasonal variation of volume transport with a maximum in the summer and a minimum in the autumn could be well reproduced by both models. The results demonstrate the wind stress component normal to a gradient vector of bottom topography is crucial for determining the seasonal variation. The similar seasonal variation widely covers the East China Sea and has a large amplitude near the Tokara Strait. Finally, it can be concluded that winds north of 35°N have little influence on the seasonal response of our model at the Tokara Strait.

1. Introduction

It has been recognized in recent years that ocean plays a critical role in the global climate system. The role of ocean in the system is divided into the following two functions, i.e. storage and redistribution of incoming heat flux from the sun. Both functions are closely related to each other. First, a large amount of heat from the sun is stored in the ocean and is slowly redistributed through ocean and atmospheric general circulations. Vonder Haar and Oort (1973) showed that ocean and atmosphere are equally important in transporting energy, the atmosphere being most important at 50°N and the ocean most important at 20°N. Western boundary currents such as the Kuroshio is considered to have played an important role in the mechanism of heat transport from a tropical region to an extra-tropical region. The transported heat energy is released for atmosphere through air-sea interaction in the mid-latitudes. For example, a large amount of turbulent heat flux can be observed south of Japan in winter because of cold and dry winter monsoon and a large difference between sea surface temperature and air temperature (e.g., Kubota and Shikauchi, 1994). This large heat flux which is carried by the Kuroshio and released over the western North Pacific may be important not only for regional climates but also global climates. Therefore, a mechanism of the variation of the Kuroshio should be understood for considering a global climate issue.

Though there have been many studies related to the transport of the Kuroshio, the accurate value of the absolute transport itself is still not clear now. However, seasonal variation of the speed and the relative transport of the Kuroshio has been reported in several papers. For example, Taft (1972) analyzed axial GEK current speed, speed from ship displacement observations and volume transport relative to 800 db and reported that a maximum appears in summer. Recently, Ichikawa and Beardsley (1993) examined the temporal and spatial variability of absolute geostrophic volume transport of the Kuroshio using hydrographic and surface current data

*Present address: Center for Climate System Research, University of Tokyo, Tokyo 153, Japan.
**Present address: Fujitsu Limited, Numazu, Shizuoka 410-03, Japan.

collected in and just outside the East China Sea. They reported that the Kuroshio volume transport is large in summer. Moreover, they pointed out that the Kuroshio volume transport is positively correlated with local downstream wind stress. The Kuroshio can be considered to be basically in geostrophic balance in which the sea-level difference is proportional to the velocity assuming hydrostatic balance. Thus, in order to monitor the Kuroshio, the sea-level difference across the Kuroshio is considered to be useful because the data can be continuously measured. In particular, the sea-level difference across the Tokara Strait such as between Naze and Nishinoomote has been considered to be important to monitor the Kuroshio because the Tokara Strait appears to be a choke point for the Kuroshio. Blaha and Reed (1982) and Kawabe (1988) studied seasonal variation of the sea-level difference across the Tokara Strait. They reported that the mean seasonal variation is at its maximum in summer and at its minimum in autumn, with a sharp decrease from summer to autumn. This sharp drop from the maximum in summer to the minimum transport in autumn is also observed for the transport of the Florida Current (e.g., Schott *et al.*, 1988). Blaha and Reed (1982) suggested Ekman pumping, particular between 11°N and 19°N determines the seasonal transport fluctuations of the Kuroshio. On the other hand, Greatbatch and Goulding (1989) recently demonstrated that the seasonal transport variations predicted by a barotropic model are very similar to those of the observed annual cycle of sea level difference across the Tokara Strait. Furthermore, Greatbatch and Goulding (1990) examined in detail the seasonal variation of the transport through the Tokara Strait by using a limited-area barotropic model of the North Pacific with a fine-resolution, 1/3° × 1/3°. They demonstrated that the inclusion of realistic bottom topography is crucial in determining the model response and the important forcing terms for their model response at the Tokara Strait are those associated with the gradients of topography and not the curl of the surface wind stress. Though they indicated important points for determining the variation of the Kuroshio transport across the Tokara Strait, the detailed mechanism of the seasonal Kuroshio variation does not seem to be so clear.

In this paper, we wish to understand a mechanism of the seasonal cycle of the sea level difference across the Tokara Strait and to clarify the area of similar seasonal variation of the model-calculated transport. The paper is organized as follows. Section 2 describes the details of the model and the forcings. Results are given in Section 3. Finally, Section 4 presents a summary and discussions.

2. The Model

The model is a linear barotropic model similar to the model of Greatbatch and Goulding (1989, 1990). We use spherical coordinate, with λ (longitude) increasing eastward and ϕ (latitude) increasing northward. The governing equations are as follows:

$$\frac{\partial u}{\partial t} - fv = -\frac{g}{a\cos\phi}\frac{\partial \eta}{\partial \lambda} + \frac{\tau^{\lambda}}{\rho_0 H} - \frac{r}{H}u + A_H\left(\nabla^2 u - \frac{1+\tan^2\phi}{a^2}u - \frac{2\sin\phi}{a^2\cos^2\phi}\frac{\partial v}{\partial \lambda}\right), \tag{1}$$

$$\frac{\partial v}{\partial t} + fu = -\frac{g}{a}\frac{\partial \eta}{\partial \phi} + \frac{\tau^{\phi}}{\rho_0 H} - \frac{r}{H}v + A_H\left(\nabla^2 v - \frac{1+\tan^2\phi}{a^2}v + \frac{2\sin\phi}{a^2\cos^2\phi}\frac{\partial u}{\partial \lambda}\right), \tag{2}$$

$$\frac{\partial}{\partial \lambda}(uH) + \frac{\partial}{\partial \phi}(vH\cos\phi) = 0 \tag{3}$$

where u and v are the current velocities in the zonal and meridional directions, η is the surface elevation, a is the radius of the Earth, H is the water depth, τ^{λ} and τ^{ϕ} are the eastward and northward components of the surface wind stress, $f = 2\Omega\sin\phi$ is the Coriolis parameter with Ω the Earth's rotation rate, g is the acceleration due to gravity, r is a linear bottom friction coefficient, ρ_0 is a density for sea water and A_H is a horizontal kinematic eddy viscosity. For the present study, we basically adopt $A_H = 10^4$ m^{2}s^{-1} and $r = 0.005$ m s^{-1}. Moreover, in order to investigate an effect of these parameters on results $A_H = 10^3$ m^{2}s^{-1} are chosen in the additional fine-mesh experiment.

Assuming the rigid-lid approximation, we can define a volume transport streamfunction ψ with

$$\psi_{\lambda} = a\cos\phi v H, \qquad \psi_{\phi} = -auH. \tag{4}$$

The vertical component of the curl of Eqs. (1) and (2) is represented in the following equation for ψ by using Eq. (4).

$$\frac{\partial}{\partial t}\left\{\frac{\partial}{\partial\lambda}\left(\frac{\psi_{\lambda}}{\cos\phi\cdot H}\right)+\frac{\partial}{\partial\phi}\left(\cos\phi\frac{\psi_{\phi}}{H}\right)\right\} \quad \text{(A) Time variation term}$$

$$= -2\Omega\sin\phi\left\{\left(\frac{\psi_{\lambda}}{H}\right)_{\phi}-\left(\frac{\psi_{\phi}}{H}\right)_{\lambda}\right\} \quad \text{(B) Topographic - } \beta \text{ term}$$

$$-2\Omega\cos\phi\frac{\psi_{\lambda}}{H} \quad \text{(C) Planetary - } \beta \text{ term}$$

$$+\frac{a}{\rho_0}\left(\tau^{\lambda}\cos\phi\frac{H_{\phi}}{H^2}-\tau^{\phi}\frac{H_{\lambda}}{H^2}\right) \quad \text{(D) Wind stress - 1 term}$$

$$+\frac{a}{\rho_0 H}\left\{\frac{\partial\tau^{\phi}}{\partial\lambda}-\frac{\partial}{\partial\phi}\left(\tau^{\lambda}\cos\phi\right)\right\} \quad \text{(E) Wind stress - 2 term}$$

$$-r\left\{\left(\frac{\psi_{\lambda}}{H^2\cos\phi}\right)_{\lambda}+\left(\frac{\psi_{\phi}\cos\phi}{H^2}\right)_{\phi}\right\} \quad \text{(F) Bottom friction term}$$

$$+\frac{A_H}{a}\left\{\frac{\sin\phi}{\cos^2\phi}u_{\lambda\lambda}-\frac{1}{\cos\phi}u_{\lambda\lambda\phi}+\frac{\sin^2\phi}{\cos\phi}u_{\phi}+2\cos\phi u_{\phi}\right.$$

$$+2\sin\phi u_{\phi\phi}-\cos\phi u_{\phi\phi\phi}+\frac{\sin\phi}{\cos^2\phi}u$$

$$+\frac{1}{\cos^2\phi}v_{\lambda\lambda\lambda}+\frac{\sin\phi}{\cos\phi}v_{\lambda\phi}+v_{\lambda\phi\phi}$$

$$\left.+\left(-1-\frac{\sin^2\phi}{\cos^2\phi}+\frac{2}{\cos^2\phi}\right)v_{\lambda}\right\}. \quad \text{(G) Lateral eddy viscosity term} \tag{5}$$

The equations are basically integrated in time using a leapfrog scheme. However, the diffusive and friction terms are computed by a forward scheme for stability (O'Brien, 1986), and the planetary-β term is computed by a trapezoidal scheme. We adopt the Arakawa C grid (Mesinger and Arakawa, 1976) to reduce computer core storage.

In the present study, two kinds of model are used. The first one, Case A is a North Pacific

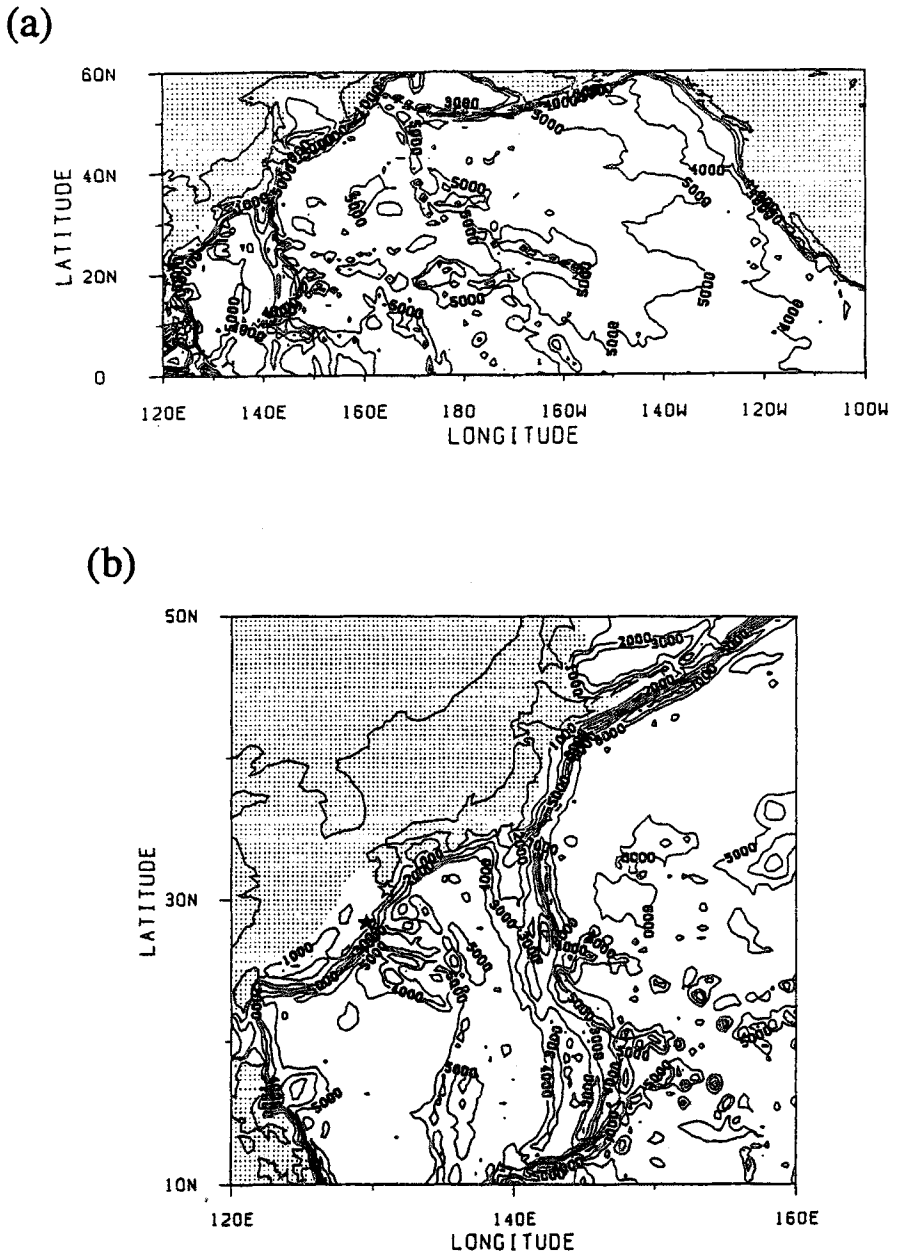

Fig. 1. The bottom topography used in the models, (a) Case A and (b) Case.B. Shaded regions mean land areas. The contour interval is 1000 m. ★ and ☆ in (b) indicate the location of Naze and Nishinoomote, respectively.

Ocean model extending from 0° to 60°N and from 120°E to 100°W and approximates the coastline geometry by using 1.0° in both directions. On the other hand, the second model, Case B is a limited-domain model bounded by latitudes 10°N and 50°N and longitudes 120°E and 160°E on a 1/3° × 1/3° grid. All boundaries are taken to no-slip solid walls in both models. The model time step is 1 hour in Case A and 20 minutes in Case B, respectively. The bottom topography used in both models are shown in Fig. 1. The wind stress fields driving the models are based on ship and buoy observations given in Comprehensive Ocean-Atmosphere Data Set (COADS) Monthly Summary Trimmed Groups (MSTG) (Slutz *et al.*, 1985). The original MSTG data of which resolution is 2° are linearly interpolated into model grid points. The density air is taken to be 1.2 kg m^{-3} and a drag coefficient is taken to be 1.5×10^{-3}.

The model is integrated from rest for 200 days by using mean wind stress for the period 1960–1979 and then integrated for two years by monthly mean wind stress. The results from the second year are used in the present analysis.

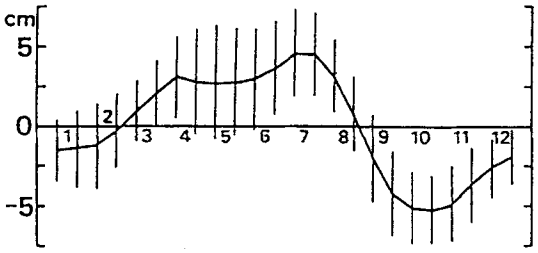

Fig. 2. Mean seasonal variations of the sea-level difference Naze minus Nishinoomote computed in each half month for 19 years from 1965 through 1983. Vertical bars show 95% confidence intervals (Kawabe, 1988).

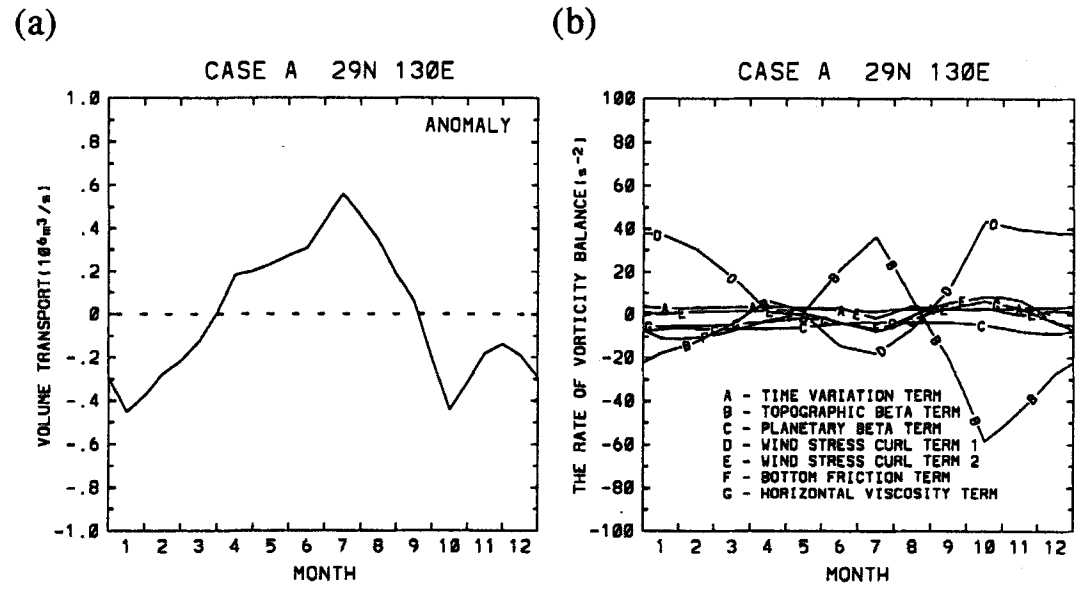

Fig. 3. Seasonal variation of (a) the anomaly of the model transport and (b) each vorticity term at 29°N, 130°E in Case A.

3. Results

3.1 Case A

Figure 2 shows the seasonal variation of the sea level difference between Naze and Nishinoomote averaged in each half month for 19 years from 1965 through 1983 (Kawabe, 1988). Kawabe (1988) reported that the sea level difference is large from March to August, small from September to February and reaches a maximum in July and minimum in October and that the sharp decrease in August and September is quite remarkable. On the other hand, the seasonal variation of the anomaly of the transport obtained from the first model at 29°N, 130°E corresponding to the location of the Tokara Straits is shown in Fig. 3(a).

The anomaly is calculated from a one-year average value. The similarity between both seasonal variations shown in Figs. 2 and 3(a) is surprisingly remarkable and is consistent with

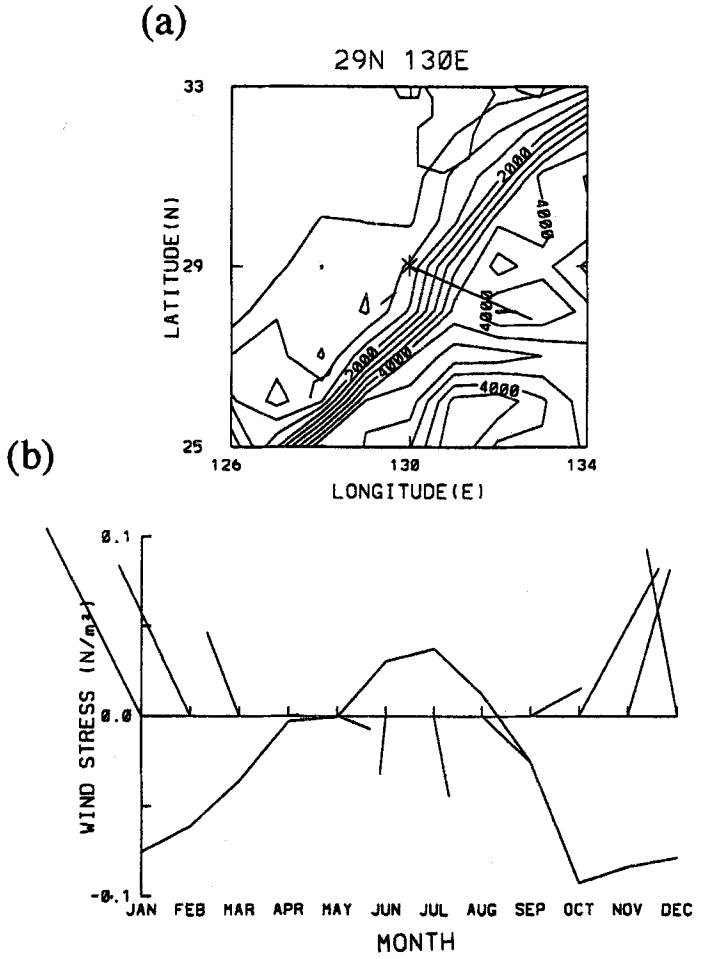

Fig. 4. (a) Bottom topography and the direction of a gradient vector, and (b) seasonal variation of the wind stress vector and the magnitude of the wind stress component along the bottom contour at 29°N, 130°E indicated by * in (a). The contour interval in Fig. 4(a) is 500 m.

the results by Greatbatch and Goulding (1990). Next, Fig. 3(b) shows a vorticity balance at the same point. It is clear from the figure that the main vorticity balance is realized between a topographic-β term and a wind stress-1 term. It should be noted that both terms are strongly associated with bottom topography. Greatbatch and Goulding (1990) demonstrated the important forcing terms for their model response at the Tokara Strait are those associated with the gradients of topography by comparing results between a model with and without bottom topography. The results shown in Fig. 3(b) are consistent with their conclusion.

Moreover, the wind stress-1 term can be rewritten in a following way.

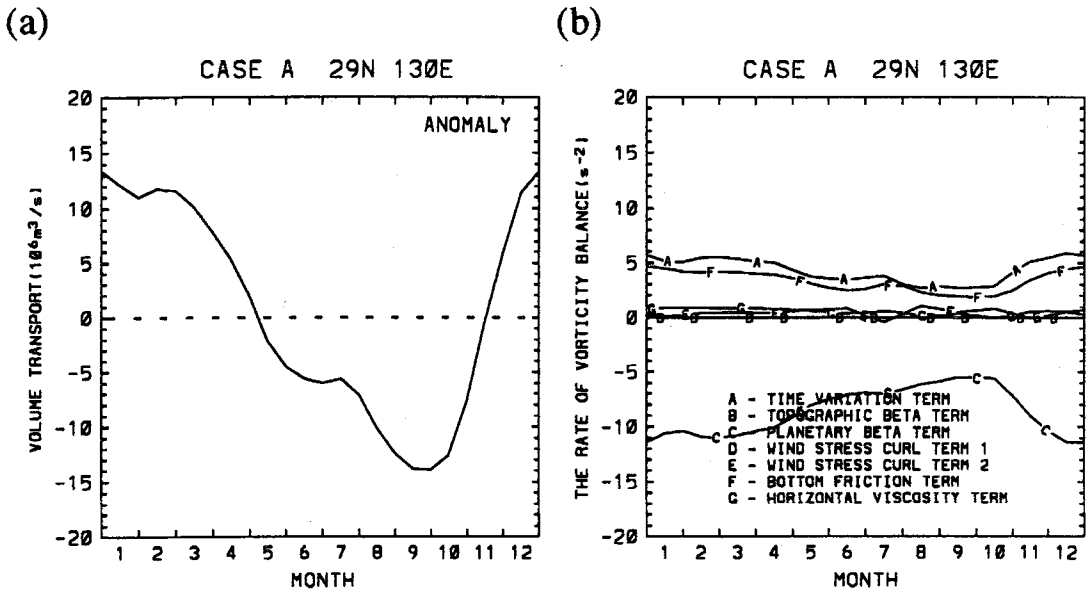

Fig. 5. Same as Fig. 3 except for a flat-bottomed model.

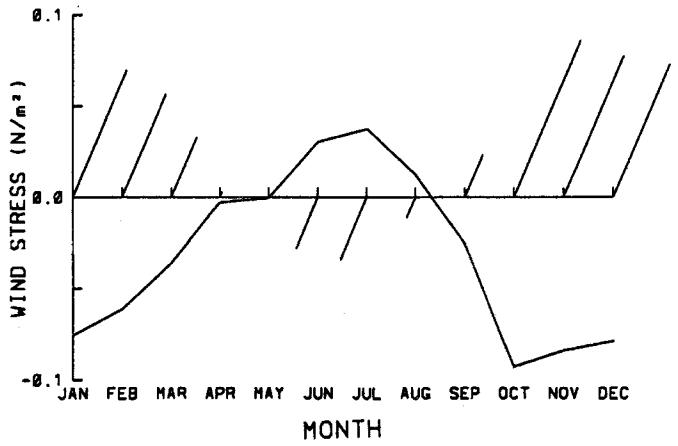

Fig. 6. Seasonal variation of the wind stress and the magnitude used in the second additional numerical experiment.

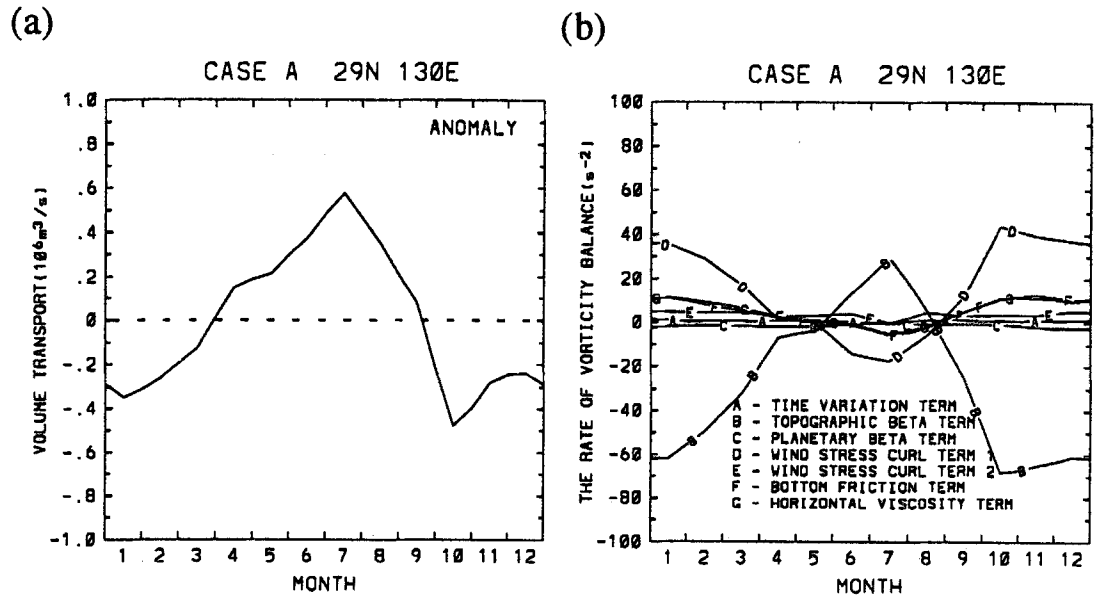

Fig. 7. Same as Fig. 3 except forced by the wind stress shown in Fig. 6.

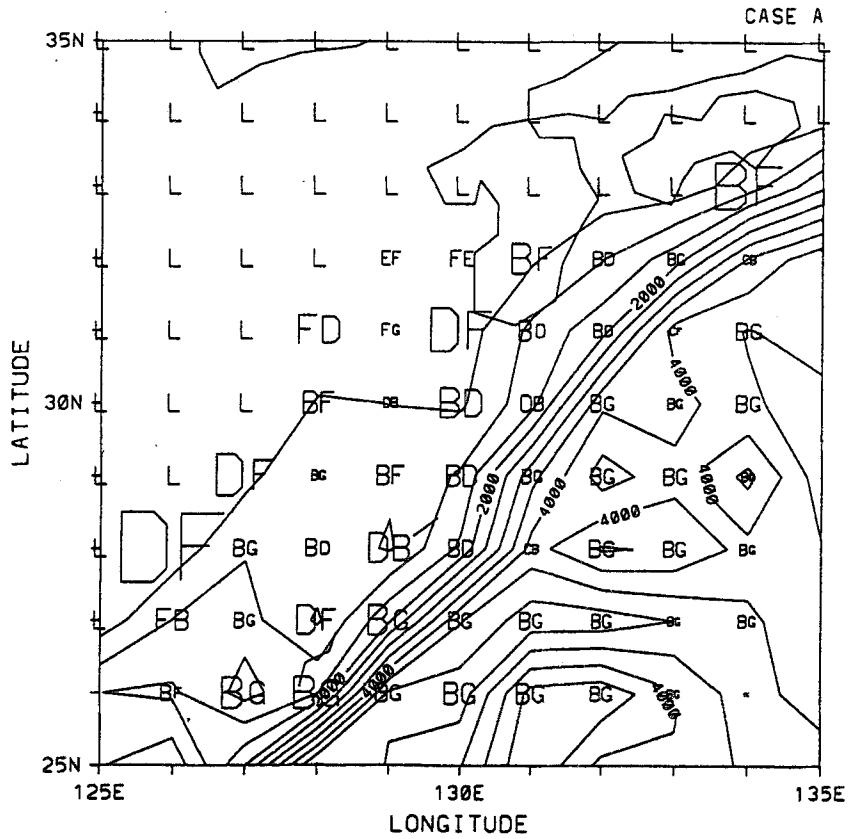

Fig. 8. The first and the second large vorticity terms at each grid point in Case A. The size indicates the magnitude of the term. "L" indicates a land area.

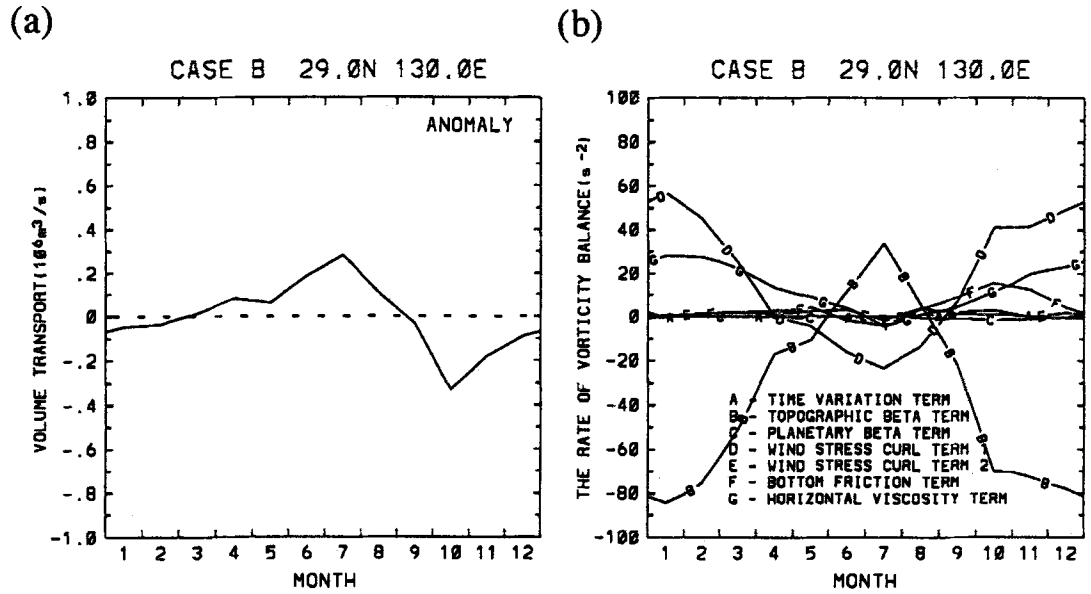

Fig. 9. Same as Fig. 3 except for Case B.

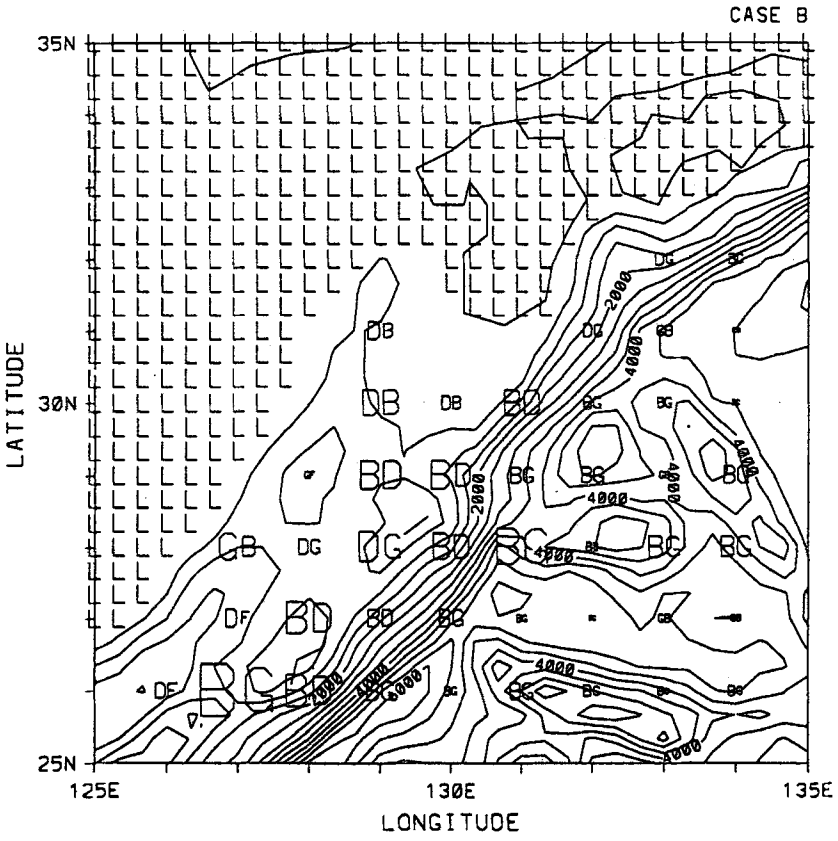

Fig. 10. Same as Fig. 8 except for Case B.

$$\frac{a}{\rho_0}\left(\tau^\lambda \cos\phi \frac{H_\phi}{H^2} - \tau^\phi \frac{H_\lambda}{H^2}\right) = \frac{a}{\rho_0 H^2}\left(\tau^\lambda \cos\phi \frac{\partial H}{\partial \phi} - \tau^\phi \frac{\partial H}{\partial \lambda}\right) = \frac{a}{\rho_0 H^2}|\vec{\tau} \times \nabla H|.$$

This representation suggests importance of the wind stress component normal to a gradient vector of bottom topography, i.e. along a bottom contour. The direction of the gradient vector of bottom topography at 29°N, 130°E is shown in Fig. 4(a). The seasonal variation of the wind stress vector and the component along the bottom contour are given in Fig. 4(b). The importance of the wind stress component along the bottom contour is demonstrated by the similarity between the seasonal variations of main terms in the vorticity equation (Fig. 3(b)) and of the magnitude of the wind stress component along the bottom contour (Fig. 4(b)). In order to recognize the importance, two additional numerical experiments are carried out. The first model is a flat-bottomed model in which the ocean depth is fixed at 4000 m. Figure 5 shows the transport is small from May to November and large from December to April. Such seasonal variation is similar to that of the Sverdrup transport shown in Sekine and Kutsuwada (1994) and quite different from that of the sea level difference across the Tokara Strait. Also, a planetary-β term is dominant in the vorticity balance (Fig. 5). Next, only the component of the wind stress along the bottom contour at 29°N, 130°E shown in Fig. 6 is used in the second experiment. Figure 7 shows the seasonal variation of the transport and each term in a vorticity equation for the second experiment. It is clearly seen that Fig. 7 is similar to Fig. 3.

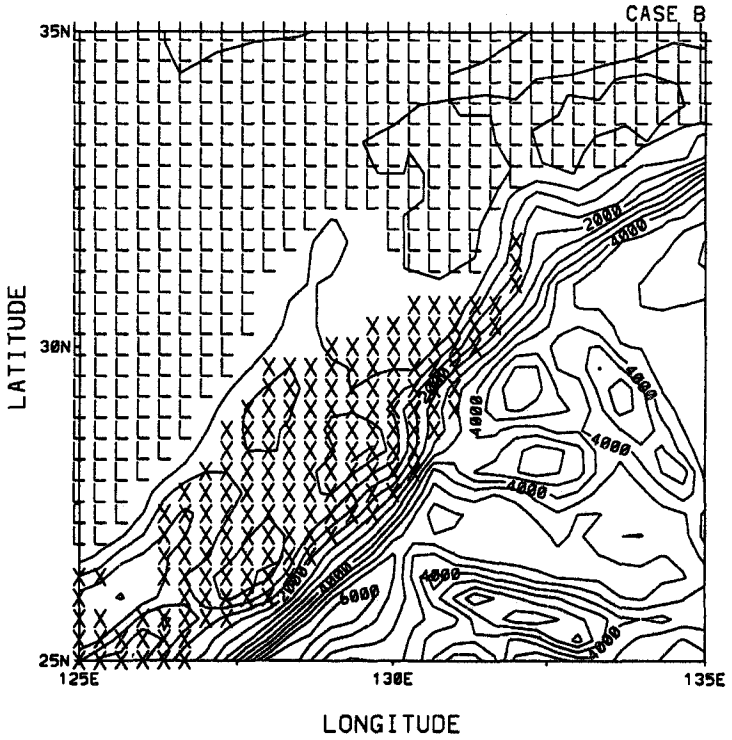

Fig. 11. The distribution of a grid point showing seasonal variation of the model-calculated transport with a maximum in summer and a minimum in winter. A cross sign indicates a location.

Vorticity balances at each grid point in the first experiment are shown in Fig. 8. The first and second large terms are given by alphabets corresponding to each term in Eq. (4). The size of an alphabet indicates a magnitude of the term. Bottom friction indicated by F is important along the boundary and the magnitudes are considerably large. On the other hand, a topographic-β term indicated by B is one of the main components off the boundary. However, the counterpart of a topographic-β term is a wind stress-1 term over the shelf region, while that is a lateral viscosity term in the open ocean and the magnitude is small. The former balance found around the Tokara Strait extends along the shelf break indicating by a 1000 m-isobath. It should be noted that the magnitude is the largest at 29°N, 130°E corresponding to the Tokara Strait.

3.2 Case B

Since the seasonal variation is a local phenomenon as Greatbatch and Goulding (1990) pointed out, the grid size (1° × 1°) used in Case A may not be suitable for detailed analysis. For example, it can be easily seen that the geometry of Kyushu Islands is not enough reproduced in Fig. 1. Therefore, next, a numerical experiment by using a limited-area model with 1/3° × 1/3° resolution is carried out.

The seasonal variation of the streamfunction at 29°N, 130°E in Case B is shown in Fig. 9(a). It is clear that the seasonal variation agrees well with that shown in Fig. 3. It is expected that a vorticity balance strongly depends on the bottom topography reproduced in the model. We therefore show a vorticity balance at each grid point in Fig. 10. We can see that the magnitudes of vorticity terms are considerably large for a shelf region such as the East China Sea and small

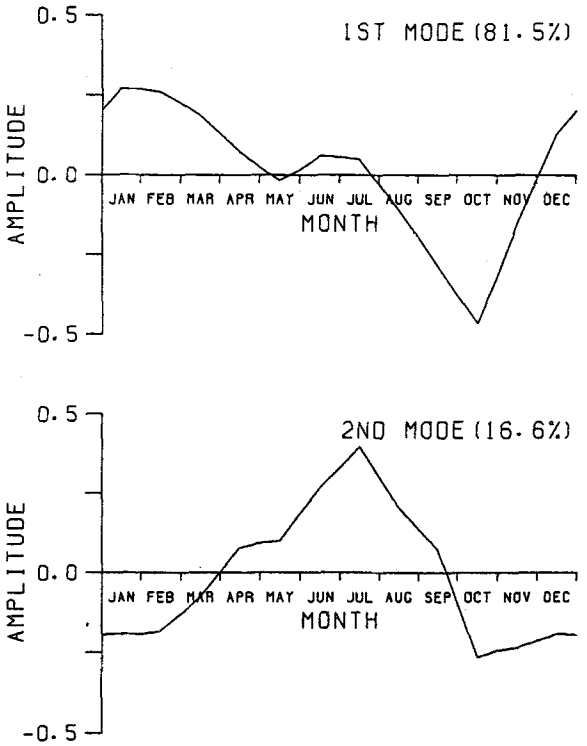

Fig. 12. Time history of amplitude functions for the first two EOFs.

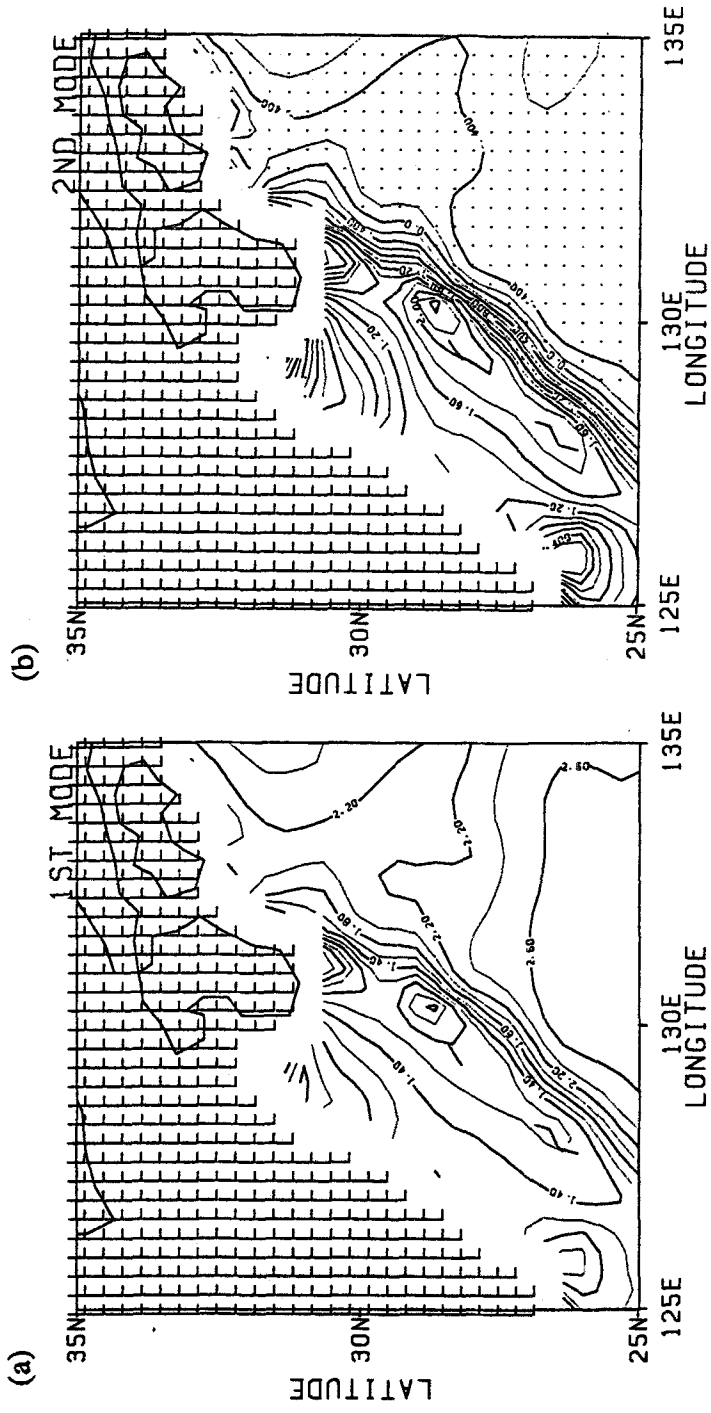

Fig. 13. Map of the eigenfunction for (a) the first mode and (b) the second mode. Shaded regions mean negative values.

for an open ocean. The distribution of a grid point showing the same seasonal variation of the transport as at 29°N, 130°E is indicated by a symbol of × in Fig. 11. It should be noted that the distribution covers a wide area compared with Fig. 8 and extends to a central region of the East China Sea. Moreover, an empirical orthogonal function (EOF) analysis was carried out for the anomaly of the streamfunction. The first two EOFs were found to explain 98.1% of the variance. The time history of amplitude functions and the eigenfunction for the first two EOFs are given in Figs. 12. and 13, respectively. The first EOF accounts for 81.5% of the variance and has a maximum in winter and a minimum in autumn. The seasonal variation may be related to that of the Sverdrup transport (Sekine and Kutsuwada, 1994). On the other hand, the second EOF has a maximum in summer and a minimum in the autumn similar to the seasonal variation of the transport at Tokara Strait. Figure 13 indicates that the seasonal variation almost covers the East China Sea and has the maximum near the Tokara Strait.

In order to easily compare these results with previous results from the North Pacific Ocean model, we adopted same values as a bottom friction and a lateral eddy viscosity coefficient. However, a smaller value may be suitable for the fine mesh model. Therefore, an additional experiment with $r = 0.005$ m s^{-1} and $A_H = 10^3$ m^{2}s^{-1} was carried out. The seasonal variation of the streamfunction at the Tokara Strait has no difference from that in the previous experiment, while the seasonal variation of each vorticity term shown in Fig. 14 is fairly different from that shown in Fig. 10. In this case, the signs of a horizontal viscosity term and a topographic-β term in winter are opposite compared with the previous case. Also, the importance of a horizontal viscosity term increases in the present case. Such a change of the vorticity balance may be caused by an increase of the Kuroshio transport shown in Fig. 15. Figure 15 indicates the transport strongly depends on the parameters related to viscosity or friction. However, it should be noted that the seasonal variation of the streamfunction at the Tokara Strait hardly depends on those parameters as mentioned before. This is consistent with results of Greatbatch and Goulding

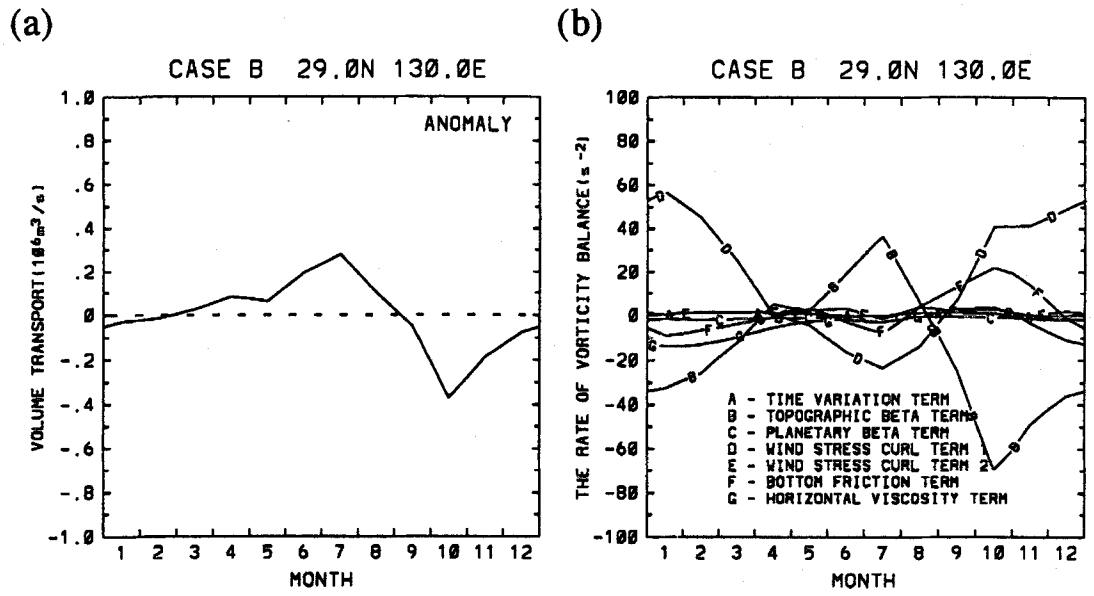

Fig. 14. Same as Fig. 10 except $A_H = 10^3$ m^{2}s^{-1}.

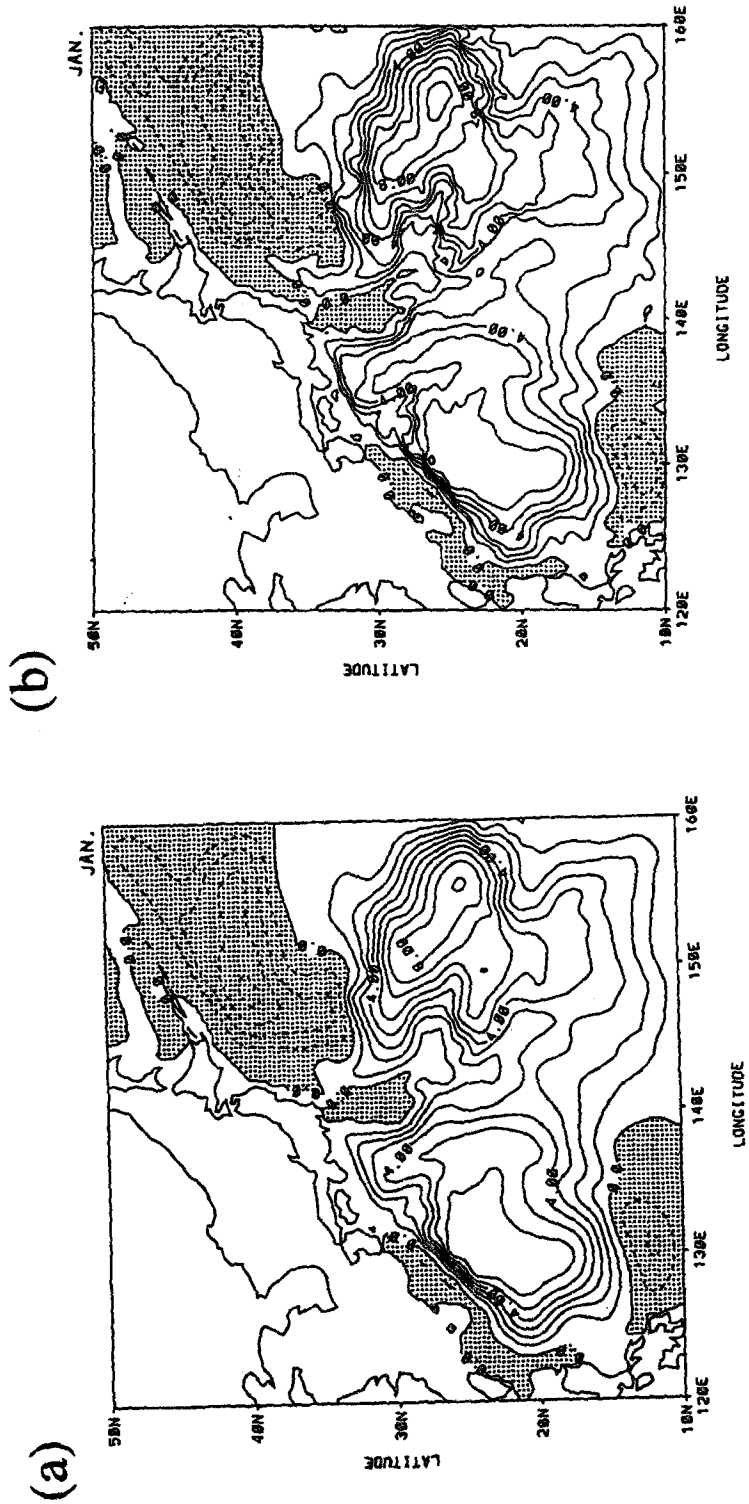

Fig. 15. Stream lines for January in the case with parameters of (a) $A_H = 10^4$ m^{2}s^{-1} and (b) $A_H = 10^3$ m^{2}s^{-1}. Shaded regions mean negative values, i.e. anticyclonic gyres. The contour interval is 1.0×10^6 m^{3}s^{-1}.

(1990) that increasing the bottom friction coefficient from 0.002 to 0.005 m s^{-1} has only a slight effect on the model-calculated transport through the Tokara Strait.

Though Fanning *et al.* (1994) indicated that the meridional component of the wind stress is the most important for determining the model-calculated seasonal transport variations at the Florida Strait, they also indicated the importance of wind forcing to the north of 35°N in their model. On the other hand, Böning *et al.* (1991) concluded that wind forcing north of 35°N is not important and wind forcing over the Caribbean/Florida Straits areas plays the major role for the seasonal transport variations at the Florida Straits. Fanning *et al.* (1994) stated that the difference between both conclusions is associated with the difference of the dynamics included in both models. In order to access an importance of wind forcing north of 35°N in our model, we conducted an experiment assuming the forcing terms (D) and (E) in Eq. (5) to be zero north of 35°N following to Fanning *et al.* (1994). However, we could find no difference between results (not shown) and the previous results for the model-calculated seasonal transport variation at the Tokara Strait. It is concluded that wind forcing north of 35°N is not important for determining the seasonal variation of the transport at the Tokara Strait in our model. It should be noted that our conclusion agrees well with that of Böning *et al.* (1991) for the Florida Current, though our model is almost same as not a Böning *et al.* (1991)'s but a Fanning *et al.* (1994)'s model.

4. Summary and Discussions

A mechanism of the variation of the sea level difference across the Tokara Strait is studied by using a linear barotropic model. The first model is a general ocean circulation model with 1° × 1° grid for the whole North Pacific Ocean, while the second model is a limited-area model with 1/3° × 1/3° grid for the western North Pacific. Both models are driven with COADS MSTG wind stress. A seasonal transport variation at the Tokara Strait calculated in both models is similar to the variation of the sea level difference across the Tokara Strait, with a maximum in the summer and a minimum in the autumn. Capability of reproducing by the limited-area model means that the variation is not a large-scale phenomenon pointed out by Blaha and Reed (1982) but a local phenomenon pointed out by Greatbatch and Goulding (1990). This may be consistent with that Kuroshio velocity in the Tokara Strait does not correlate with the position of the Kuroshio axis over the Izu Ridge (Kawabe, 1988). Accordingly, it should be noted that monitoring of the Kuroshio transport at the Tokara Strait by using the sea level difference does not mean monitoring of the transport of the subtropical gyre. It can be seen that the seasonal variation of the model-calculated transport at the Tokara Strait strongly depends on the wind stress component along the local depth contour. The cross product of the wind stress vector with the gradient vector of ocean depth basically plays an important role in the vorticity balance near the Tokara Strait. This is consistent with observational results from Ichikawa and Beardsley (1993) who indicated that the Kuroshio volume transport is positively correlated with local down stream wind stress.

The EOF analysis was carried out for the streamfunction in limited-area model. The first mode corresponds to the Sverdrup transport, while the second mode corresponds to the seasonal variation of the transport through the Tokara Strait. The map of the eigenfunction of the second mode shows the remarkable seasonal variation with a maximum in summer and a minimum in autumn found in the model-calculated transport at the Tokara Strait almost extends over the East China Sea. This distribution is supported by observational results that the Kuroshio volume transport is large in summer (Ichikawa and Beardsley, 1993).

The Florida Straits are choke points for the Florida Current and supposed to be a counterpart

of the Tokara Strait. Seasonal transport variations through the Florida Straits have been studied in the past years. Niiler and Richardson (1973) found out that the observed seasonal transport variation is out of phase with that of the flat-bottomed Sverdrup transport. Schott *et al.* (1988) and Lee and Williams (1988), pointed out that the annual transport cycle of the Florida Current shows great similarity with the annual cycle of the along-channel wind stress component and suggested that the seasonal change in along-channel wind forcing provides a significant contribution to the annual transport cycle of the Florida Current. Furthermore, Böning *et al.* (1991) studied seasonal transport variation in the western subtropical North Atlantic by using the high-resolution model of the wind-driven and thermohaline circulation developed by Bryan and Holland (1989). They showed the annual variation of the transport through the Florida Straits, with a maximum in summer and a minimum in autumn in their model. They also noted that the seasonal variation of the Florida Current is mainly forced by the meridional component of the wind stress in the vicinity of the straits. Furthermore, they claimed that winds north of 35°N have little influence on the seasonal response of their model at the Florida Straits. Our results suggest that the annual variation of the transport through the Tokara Strait also can be explained by a local theory such as that through the Florida Straits. Recently, Fanning *et al.* (1994) investigated the response at the Florida Straits by using the similar model to our model, i.e. a linear, barotropic model at 1° × 1° resolution. They decompose their model response at the Florida Straits into parts associated with each of the forcing term as well as in the present study. Their results also showed the importance of the wind stress-1 term, especially associated with the meridional component of wind stress in conjunction with longitudinal gradients of topography, for the model response at the Florida Straits, which is very similar to our results for that at the Tokara Strait. However, Fanning *et al.* (1994) concluded that winds north of 35°N play an important role for the seasonal response of their model at the Florida Straits instead of local theory suggested by Lee and Williams (1988) and Böning *et al.* (1991). Fanning *et al.* (1994) indicated that the discrepancies between results from Böning *et al.* (1991) may be due to nonlinear effects by advection which was not included in their model. If the discrepancies are caused by nonlinear effects, a mechanism of the seasonal variation of the transport at the Florida Straits should be different between results from Böning *et al.* (1991) and Fanning *et al.* (1994). Whether similar discrepancy exists or not for that at the Tokara Strait is unknown. This point should be clarified in the future study.

Sekine and Kutsuwada (1994) recently investigated the seasonal variation in volume transport of the Kuroshio south of Japan. Their model is a two-layer model with a 1° × 1° driven by the observed wind stress compiled by Kutsuwada and Teramoto (1987). The seasonal variation of the Kuroshio volume transport is quite different from that of the sea level difference across the Tokara Strait, while that of the vertical velocity-difference has a maximum in summer and a minimum in autumn similar to that of the sea level difference across the Tokara Strait. Since the volume transport and a vertical velocity-difference are estimated as the mean value over the fairly wide band region in their study, the relation between their results and the seasonal variation of the sea level difference across the Tokara Strait is not clear. On the other hand, the amplitude of the seasonal variation in volume transport through the Tokara Strait cannot be well reproduced in the present study. Greatbatch and Goulding (1990) pointed out the possibility of increasing the amplitude of the seasonal signal if the density stratification and a representation of the mean flow of the Kuroshio. Considering that the seasonal variation of the sea level difference across the Tokara Strait can be reproduced by the simple barotropic model, it may be expected that energy transfer from a barotropic mode to a baroclinic mode locally occurs by the JEBER effect (Huthnance, 1984). This may be a future problem.

We focused on seasonal variation of the sea level difference and the model-calculated transport in the present study. However, there are many studies to point out interannual variation of the Kuroshio transport and the sea level difference across the Tokara Strait. It can be easily imagined an importance of a baroclinic mechanism for interannual variation of the Kuroshio because of the long time scale of a baroclinic response. However, Kutsuwada (1988) pointed out that interannual variation in sea level difference across the Tokara Strait is coherent with that of the zonally-integrated Sverdrup transport in the latitudinal zone along 30°N. His result suggests that the interannual variation of the Kuroshio transport at the Tokara Strait can be explained by the barotropic response to the wind stress. Investigation of this problem is now being made by using a present model.

Acknowledgements

We thank I. Yasuda for the valuable assistance with development of the model code and stimulating discussions. The computations were carried out using the FACOM VP-50E at Tokai University.

References

Blaha, J. and R. Reed (1982): Fluctuations of sea level in the western North Pacific and inferred flow of the Kuroshio. *J. Phys. Oceanogr.*, **12**, 669–678.

Böning, C. W., R. Döscher and R. G. Budich (1991): Seasonal transport variation in the western Subtropical North Atlantic: Experiments with an eddy-resolving model. *J. Phys. Oceanogr.*, **21**, 1271–1289.

Bryan, F. O. and W. R. Holland (1989): A high resolution simulation of the wind- and thermohaline driven circulation in the North Pacific Ocean. Parameterization of Small-Scale Processes. p. 99–115. In *Proc. 'Aha Huliko'a, Hawaiian Winter Workshop*, ed. by P. Müller and D. Henderson, University of Hawaii at Manoa.

Fanning, A. F., R. J. Greatbatch, A. M. Da Silva and S. Levitus (1994): Model-calculated seasonal transport variations through the Florida Straits: A comparison using different wind-stress climatologies. *J. Phys. Oceanogr.*, **24**, 30–45.

Greatbatch, R. J. and A. Goulding (1989): Seasonal variation in a linear barotropic model of the North Pacific driven by the Hellerman and Resenstein wind stress field. *J. Geophys. Res.*, **94**, 12,645–12,665.

Greatbatch, R. J. and A. Goulding (1990): On the seasonal variation of transport through the Tokara Strait. *J. Oceanogr.*, **46**, 9–20.

Huthnance, J. M. (1984): Slope currents and "JEBER". *J. Phys. Oceanogr.*, **14**, 795–810.

Ichikawa, H. and R. C. Beardsley (1993): Temporal and spatial variability of volume transport of the Kuroshio in the East China Sea. *Deep-Sea Res.*, **40**, 583–605.

Kawabe, M. (1988): Variability of Kuroshio velocity assessed from the sea-level difference between Naze and Nishinoomote. *J. Oceanogr.*, **44**, 293–304.

Kubota, M. and A. Shikauchi (1994): Sensible and latent heat flux in the North Pacific using satellite data. p. 55–60. In *Proc. PORSEC-94*.

Kutsuwada, K. (1988): Interannual correlations between sea level difference at the south coast of Japan and wind stress over the North Pacific. *J. Oceanogr.*, **44**, 68–80.

Kutsuwada, K. and T. Teramoto (1987): Monthly maps of the surface wind stress fields over the North Pacific during 1961–1984. *Bull. Ocean Res. Inst., University of Tokyo*, **24**, 100 pp.

Lee, T. N. and E. Williams (1988): Wind forced transport fluctuations of the Florida Current. *J. Phys. Oceanogr.*, **18**, 937–946.

Mesinger, F. and A. Arakawa (1976): Numerical methods used in atmospheric models, GARP Pub. ser. 17, Vol. 1, World Meteorol. Organ., Geneva, 64 pp.

Niiler, P. P. and W. S. Richardson (1973): Seasonal variability of the Florida Current. *J. Mar. Res.*, **31**, 144–167.

O'Brien, J. J. (1986): The diffusive problem. p. 127–144. In *Advanced Physical Oceanographic Numerical Modelling*, ed. by J. J. O'Brien, D. Reidel, Norwell, Mass.

Schott, F. A., T. N. Lee and R. Zantopp (1988): Variability of structure and transport of the Florida Current in the period range from days to seasonal. *J. Phys. Oceanogr.*, **18**, 1209–1230.

Sekine, Y. and K. Kutsuwada (1994): Seasonal variation in volume transport of the Kuroshio south of Japan. *J. Phys. Oceanogr.*, **24**, 261–272.

Slutz, R. J., S. J. Lubker, J. D. Hiscoz, S. D. Woodruff, R. L. Jenne, D. H. Joseph, P. M. Steurer and J. D. Elms (1985): Comprehensive Ocean-Atmosphere Data Set; Release 1a, NOAA Environmental Research Laboratories, Climate Research Program, Boulder, CO., 268 pp. (NTIS PB86-105723).

Taft, B. A. (1972): Characteristics of the flow of the Kuroshio south of Japan. p. 165–216. In *Kuroshio*, ed. by H. Stommel and K. Yoshida, University of Washington Press, Washington.

Vonder Haar, T. H. and A. H. Oort (1973): New estimate of annual poleward energy transport by northern hemisphere oceans. *J. Phys. Oceanogr.*, **3**, 169–172.